

Erratum to: Nonsmooth Mechanics

Erratum to: B. Brogliato, *Nonsmooth Mechanics*, Communications and Control Engineering,

DOI [10.1007/978-3-319-28664-8](https://doi.org/10.1007/978-3-319-28664-8)

The original version of the book was inadvertently published with incorrect text, figures and equations. The incorrect text, figures and equations were corrected. The erratum chapters and the book have been updated with the changes.

- Page 21: Figure 1.3 (b) has a severe shortcut in the right curved arrow indicating “Yosida approximation”. A better view of the transformations is depicted in Figure 1 below. In the same vein it is worth reading [1].
- Page 49, Section 1.4.3.1: other studies using the Zhuravlev-Ivanov nonsmooth transformation may be found in [3–6].
- Pages 71-72: A first comment is that the damping coefficients that incorporate e_n (as those listed page 71), may be seen as extensions to the nonlinear spring-dashpot model, of (2.9) page 56 which also involves the CoR. We note that in reference 1220, the coefficient p in (2.24) is found heuristically to be $p = \frac{1}{4}$. Thus their model has a dissipative force equal to $\alpha\sqrt{mK_h}x^{\frac{1}{4}}\dot{x}$ if x is the normal indentation, with $\alpha = -\ln(e_n)\sqrt{\frac{5}{\pi^2 + \ln(e_n^2)}}$ (compare with the expression in (2.9) dropping km outside the parantheses). In [7] it is proposed to enlarge the right-hand side of (2.24) to $-\gamma x(t)^p \dot{x}(t) - kx(t)^w$, and γ is chosen as $\alpha m \dot{x}(t_0) \left(\frac{k}{m \dot{x}(t_0)^2}\right)^{\frac{1+p}{1+w}}$. They find that $p = \frac{1-w}{2}$ yields $\alpha = -\ln(e_n)\sqrt{\frac{2(1+w)}{\pi^2 + \ln(e_n)^2}}$. According to [7, Figure 2], their model has a loading-unloading curve similar to Figure 2.4 (a) page 70, with no negative contact force near zero indentation. Several nonlinear spring-dashpot models (Kuwabara-Kono, Hu et al, Tsuji et al) are further compared in [8] in terms of variation of e_n with respect to the damping coefficient, acceleration histories, acceleration/indentation loading/unloading curves, *etc*, for the case of two spheres colliding. Then

The updated original online version for this book can be found at [10.1007/978-3-319-28664-8](https://doi.org/10.1007/978-3-319-28664-8)

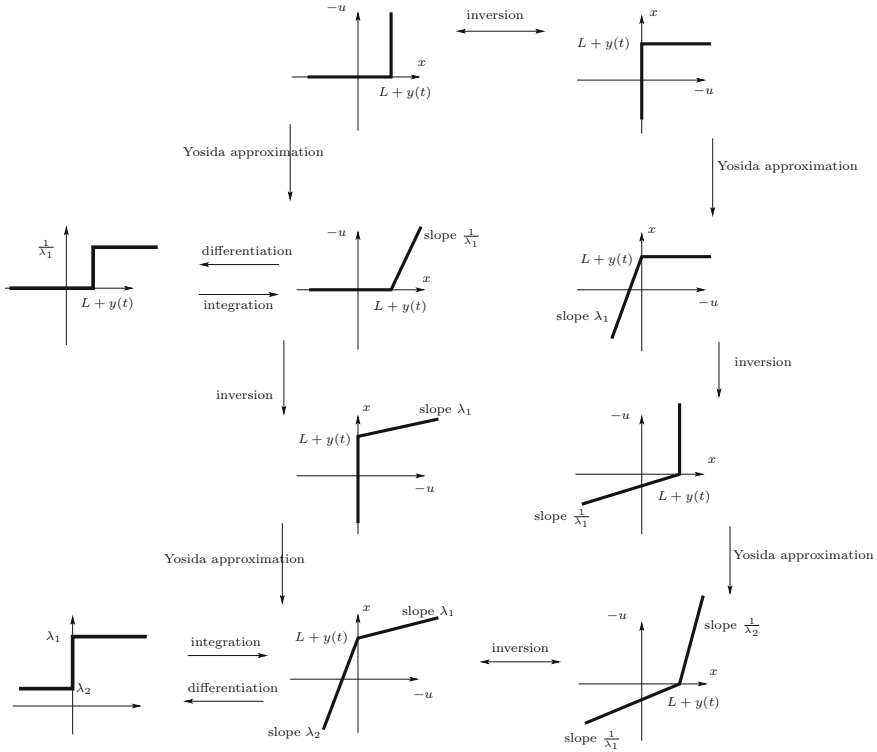


Fig. 1 Enhanced Fig. 1.3 (b)

[8] investigates the influence of the spring-dashpot models on a multiple impact process in a chain of aligned balls. To this aim they rely on the experimental data in reference 625. In particular [8, Figure 11] is exactly Figure 20 in [9] (reference 928) and Figure 29 in [10] (reference 629), where the numerical results are obtained with the LZB model (section 6.3). More work is necessary to determine the domains of validity (in terms of applications, ease of numerical simulation, etc) of these models.

- Page 75: footnote 21 should be on page 74, at the end of the framed paragraph.
- Page 99, line 5: replace (B.5) by (B.6). The calculations after (3.13) are in fact the proof in this particular case, that the normal cone can also be written as in (B.5) page 549.
- Page 102, line -5: replace $n_i \in \mathbb{R}^3$ by $n \in \mathbb{R}^3$ (the subscript i in $F_{n,i}$ refers to the contact point number).
- Page 103, line 4: $\mathcal{P}_i = v_{n,i} F_{n,i} = \dots$
- Page 113: Equation (3.41) is obtained assuming that at an impact instant all virtual displacements and velocities are allowed. This indeed results in zero impact because $M(q(t_k))(\dot{q}(t_k^+) - \dot{q}(t_k^-)) = 0 \Rightarrow \dot{q}(t_k^+) - \dot{q}(t_k^-) = 0$ (the mass matrix is assumed to be full rank). In reference 724 it is supposed that the generalized momentum satisfies $p(t_k^+) - p(t_k^-) \in -N_\Phi(q(t_k))$, as a modelling assumption since constraints are perfect during impacts (see (iii) page 104). It is shown in reference 724 that this inclusion is equivalent to the variational inequality $\langle p(t_k^+) - p(t_k^-), \bar{\delta}_q \rangle \geq 0$ for all $\bar{\delta}_q \in T_\Phi(q(t_k))$,

where the virtual displacements $\bar{\delta}_q$ are continuous (we can therefore see these developments as the extension of the material in (3.13) and below, to the case with elastic impacts). This equivalence is not surprising when we consider the normal cone definition in (B.5), recalling that this definition remains true even for nonconvex sets, see Remark B.1 page 550. Using that $p(t) = M(q(t))\dot{q}(t)$ and Moreau's set inclusion in Section B.2.2, we may impose the stricter inclusion $M(q(t_k))(\dot{q}(t_k^+) - \dot{q}(t_k^-)) \in -N_{T_{\Phi}(q(t_k))}(\dot{q}(t_k^+))$ which is equivalently rewritten as the variational inequality: find $\dot{q}(t_k^+) \in T_{\Phi}(q(t_k))$ such that $\langle M(q(t_k))(\dot{q}(t_k^+) - \dot{q}(t_k^-)), v - \dot{q}(t_k^+) \rangle \geq 0$ for all $v \in T_{\Phi}(q(t_k))$ (see (5.53) and (5.60) in Section 5.2). Thus we obtain this time the extension of (3.7) where virtual velocities are considered, and the extension of (5.45) for the case of impacting motions. We note in passing that the arguments that yield [13, Equation (1a)] (which is the same as $p(t_k^+) - p(t_k^-) \in -N_{\Phi}(q(t_k))$ with missing mass matrix and minus sign in the right-hand side) are spurious: there is a shortcoming in the reasoning in [13] because of the use of the condition $\delta_q(t_k) + \dot{q}(t_k)\delta t_k \in T_{q(t_k)} \text{bd}(\Phi)$, while $\dot{q}(\cdot)$ jumps at t_k , and $T_{q(t_k)} \text{bd}(\Phi)$ denotes the tangent plane at $q(t_k)$ (and not the tangent cone) to the boundary of the admissible domain (the correct way to derive the material page 385 in [13], is in Section 6 of reference 724 by Leine et al).

The above basic assumption yields Theorem 3 in reference 724 which is a Hamilton principle in strong norm, or strong Hamilton principle. There exists a weak norm for a weak Hamilton's principle which somewhat relaxes the assumption on the generalized momenta at impact times, see Theorem 4 and condition (99) in reference 724.

- Page 130, about the calculation of the normal and tangential vectors at the contact point A (local kinematics): the starting point is that if a 3D surface is defined by two parameters u and v and a differentiable function $r(u, v), r: \mathbb{R}^2 \rightarrow \mathbb{R}^3$, then $\frac{\partial r}{\partial u}(u_1, v_1) \in \mathbb{R}^3$ and $\frac{\partial r}{\partial v}(u_1, v_1) \in \mathbb{R}^3$ span the tangent plane at the point A_1 parameterized by u_1 and v_1 , and one can then define the normal vector as the cross product $\mathbf{n}_1 = \frac{\partial r}{\partial u}^T(u_1, v_1) \times \frac{\partial r}{\partial v}^T(u_1, v_1)$ (one should take care of the correct order to get the right orientation of the normal).
- Page 133, about the time-derivative of the right-hand side of (4.17): Let us denote the Galilean frame as $\mathcal{L}_0 = \mathcal{G}$ and the local frame as \mathcal{L} . The angular velocity vector between both frames is denoted as $\Omega_{\mathcal{L}/\mathcal{L}_0}$. We obtain $\frac{d}{dt}[(A_2A_1)^T \mathbf{n}] = \frac{d}{dt}[(A_2A_1)^T] \mathbf{n} + (A_2A_1)^T \frac{d}{dt} \mathbf{n}$. Assume that the vectors are expressed in \mathcal{L}_0 . Then basic kinematics say that $\frac{d}{dt} \mathbf{n} = \frac{d}{dt} \mathbf{n}|_{\mathcal{L}} + \Omega_{\mathcal{L}/\mathcal{L}_0} \times \mathbf{n} = \Omega_{\mathcal{L}/\mathcal{L}_0} \times \mathbf{n}$ since \mathbf{n} is constant in \mathcal{L} . Thus $(A_2A_1)^T \frac{d}{dt} \mathbf{n} = (A_2A_1)^T (\Omega_{\mathcal{L}/\mathcal{L}_0} \times \mathbf{n}) = 0$ since the vector product is orthogonal to \mathbf{n} and the vector (A_2A_1) is along \mathbf{n} . Therefore $\frac{d}{dt}[(A_2A_1)^T \mathbf{n}] = \frac{d}{dt}[(A_2A_1)^T] \mathbf{n}$. The vector $\frac{d}{dt}[(A_2A_1)^T]$ is the time derivative of (A_2A_1) in \mathcal{L}_0 and may be named the relative velocity between both bodies. The sentence "In particular..., except if \mathbf{n} is fixed in \mathcal{G} " is meaningless and should be deleted. It becomes true if stated in terms of the acceleration $\frac{d}{dt} V_{A_i}$ and $\dot{v}_{i,n}$.
- Page 162, Section 4.2.3 (also page 169, section 4.2.5.2): [25] study the force/indentation relation $f(\delta) = k\delta^n$ for an elastic body with a rough surface in contact with a rigid flat surface. A three-dimensional rough surface is constructed using a modified two-variable Weierstrass-Mandelbrot fractal function. Results in [25, Table 2] show that n can vary between 2.11 and 1.19 depending on some parameters (like fractal dimension, fractal roughness, root-mean-square roughness and arithmetic average height R_a). Thus the elasticity is found to be superlinear and even sometimes super-Hertz. Compared with the study described in Section 4.2.3 where $n = 1$ in (4.61), it seems that surface roughness increases n . The interest of

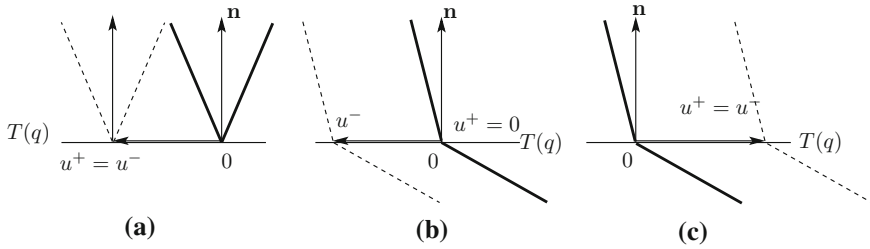


Fig. 2 Sweeping process with friction

such study is to show that Hertz' fundamental assumption (ii) page 147 (introduction of Section 4.2.1.1) on smooth contacting surfaces, may play a role in the elasticity coefficient. However we should also note that the surfaces in contact considered in [25] are conforming in addition to be rough, and that contrary to (4.61) the flat is considered non-deformable.

- Page 164, Section 4.2.4: see a comment below (page 384).
- Page 165: Hurmuzlu's analysis of the micro-impact phenomenon (Section 4.3.10.2) seems to contradict Love's criterion, because micro-collisions excite transversal modes in the beam (page 228) and these vibrations dissipate energy.
- Pages 165-166: estimations of the CoR for harmonic chains of aligned beads colliding a wall, and taking into account sequences of repeated impacts as well as the vibrational energy trapped in the chain, are given in [28, 29].
- Page 200, Equation (4.124): the last term is $\frac{dp}{dt}$.
- Page 245, line 6: $\dots + w_b(q, \dot{q}, t)$.
- Pages 247-248, Proposition 5.3: The equality $h(t') - h(t) = \int_t^{t'} \dot{h}(s) ds$ used in the proof means that $h(\cdot)$ is absolutely continuous (not just continuous) and that what is denoted as $\dot{h}(\cdot)$ is its almost-everywhere derivative. The same holds for (ii), where $\dot{h}(\cdot)$ has to be absolutely continuous as well.
- Page 270, line above (5.61): [780, 781].
- Page 280, in Theorem 5.3, line 3: replace $T_\Phi(q(t_0))$ by $V(q(t_0))$, as it is not guaranteed in general that both tangent cones are equal. Same page 282 in Remark 5.13.
- Page 286, about Coulomb's friction: notice that in the sliding mode one has $\|F_t\| = \alpha \|v_t\| = \mu \|F_n\| \Leftrightarrow \alpha = \frac{\mu \|F_n\|}{\|v_t\|}$. Hence we recover the equivalent classical way of expressing sliding Coulomb's friction as $F_t = -\mu \|F_n\| \frac{v_t}{\|v_t\|}$.
- Page 293, line 5: $\dots \operatorname{sgn}(\ddot{x}(t^+))$ when $\dot{x}(t) = 0, \dots$
- Page 295: in case of non trivial mass matrix, Equation (5.97) becomes $u(t_k^+) = \operatorname{proj}(0, [u(t_k^-) + M(q(t))^{-1} \mathcal{C}(q(t))] \cap T(q(t))$ [15]. Proposition 3.3 in [16] extends (5.97), and Figure 5.12 which depicts the algorithm in case of a trivial mass matrix. Additional figures which complete Fig. 5.12 page 295, are in Figure 2. Case (a) shows that if the mass matrix is trivial (the identity matrix) then when $u(t^-)$ is tangent to the constraint boundary, there is no velocity jump (no impact without collision). Case (b) shows that when the mass matrix is not trivial and the generalized friction cone dips below the tangent hyperplane, then the velocity may jump. But case (c) shows that depending on the tangent velocity signum, the velocity may remain continuous. It is noteworthy that the zero vector in (5.97) refers to velocities, not positions.
- Page 298, last line: replace $x_{2,n}$ by $(A_2 A_1)^T \mathbf{n}$.

- Page 299, more details about P-matrices and the difference with positive definite matrices. *Principal minors* are the determinants of the principal submatrices, they are sometimes also called *principal subdeterminants*. *Principal submatrices* of a matrix $M \in \mathbb{R}^{n \times n}$ are constructed as follows: let the index set $\mathcal{I} = \{1, 2, \dots, n\}$, and consider any subset $\mathcal{J} \subseteq \mathcal{I}$. Let us denote $\mathcal{J} = \{i_1, i_2, \dots, i_m\}$, with $m \leq n$, and $i_k \in \mathcal{I}$ for all $1 \leq k \leq m$. Delete all rows and columns of M which are indexed by i with $i \notin \mathcal{J}$. The obtained matrix $M_{\mathcal{J}} \in \mathbb{R}^{m \times m}$ is a principal submatrix of M . A *leading principal submatrix* of M is obtained by considering $i_k = k, k = 1, 2, \dots, m$. The determinant of a leading principal submatrix is a *leading principal minor*.

Theorem 5.5 states that a P-matrix has to have all its principal submatrices with positive determinant, *i.e.* all positive principal minors. A (real) matrix M (nor necessarily symmetric) is positive definite if and only if $M^T + M$ has all its leading principal minors positive (and also its leading principal submatrices are positive definite matrices). If in addition $M = M^T$, then $M \succ 0$ if and only if all its principal minors are positive (and another characterization is: if and only if all its leading principal minors are positive, showing in passing that a positive definite matrix is a P-matrix). A (real) matrix M (nor necessarily symmetric) is positive semidefinite if and only if $M^T + M$ has all its principal minors non negative. Thus for positive definiteness it is sufficient to check the leading principal submatrices, while for positive semi definiteness all principal submatrices have to be checked.

Another characterization of P-matrices is as follows [2, Lemma 16, Theorem 59]: if M is a P- matrix, the inequalities $Mx \leq 0$ and $x \geq 0$ have only the trivial solution $x = 0$. Also there exists $x > 0$ such that $Ax > 0$.

- Section 5.4.2: I said nothing on *cone linear complementarity problems* of the form $K \ni z \perp w = Mz + r \in K^*$ where K is a closed convex cone. See Theorem 8 and Corollary 5 in reference 23 for the existence of solutions to CLCP.
- Section 5.4.2. Another result that completes this section concerns the number of solutions to LCPs for which uniqueness fails. This is tackled in [14]. A matrix is said to be an \mathcal{N} -matrix if its all principal minors are negative. For such matrices, the LCP (5.105) has either 0, 1, 2 or 3 solutions. A solution z^* is degenerate if $z_i^* = 0$ and $w_i = (Mz^*)_i + r_i = 0$ for some i .

Lemma 1 [14, Lemma 2.4, Theorem 3.2, Theorem 3.3, Theorem 3.4] (i) Let M be an \mathcal{N} -matrix and $M \prec 0$. Then for each $r \geq 0$, the LCP in (5.105) has a solution, and has no solution for $r \not\geq 0$ (componentwise inequality). The LCP has exactly two solutions for $r > 0$. (ii) Let M be an \mathcal{N} -matrix and $r \in \mathbb{R}^n$. Then if M is not negative definite and $r \not\geq 0$, the LCP (5.105) has a unique solution. (iii) Let M be an \mathcal{N} -matrix, non negative definite, and $r > 0$. Then if all solutions of the LCP (5.105) are non degenerate, the LCP has exactly three solutions. Otherwise it has exactly two solutions. (iv) Let M be an \mathcal{N} -matrix, non negative definite, and $0 \neq r \geq 0$, with $r_i = 0$ for some i . Then the LCP (5.105) has exactly two solutions, with one solution degenerate.

- Page 313: replace $u_2(t) - u_1(t)$ by $u_2(t)$, and replace $u_2(t)$ by $u_2(t) - u_1(t)$, in the dynamical equations (5.130).
- Pages 320–321: further studies on the stability of nonsmooth circuits (characterization of equilibria, Lyapunov stability) may be found in [20, 21].
- Page 322: in the paragraph after Theorem 5.12: $\mathcal{E} > 0$.
- Page 323: in (5.150) it happens that $V(t^+) - V(t^-) \leq 0$ provided that $0 \in S(t)$, with $S(t)$ in (5.139). See reference 480, Lemma 3.
- Page 328, line 1: delete the “and”.

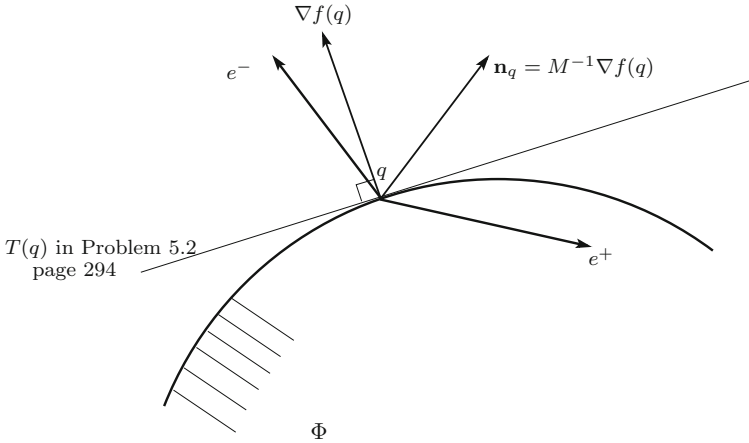


Fig. 3 Painlevé paradox and generalized friction cone

- Page 332, Proposition 5.24 and Equation (5.158): the matrix $P^\mu(q)$ is defined as

$$-\nabla f(q)^T M(q)^{-1} H_{t,u}(q) [\mu_i \operatorname{sgn}(\nu_{t,u,i})].$$

- Page 352, Section 5.6.4. Mathematical results on the existence of solutions (velocity $u(\cdot)$ of local bounded variation, $q(t) = q(0) + \int_0^t u(s) ds$) which extend results in both references 867 and 1141, 1142, can be found in [15, 16]. It incorporates Painlevé paradoxes, in the sense that the generalized friction cone may dip below the tangent cone boundary at the considered contact point (as pointed out in footnote 31 page 295, and in a paragraph above Figure 5.24 page 353). An example of calculation of the generalized friction cone for the Painlevé sliding rod system, may be found in [17, Section 2.2]. Using the notation of Equation (5.1) and of Section 6.2, the Painlevé sliding rod example of Section 5.6.1 may be written as $\ddot{q} = \mathbf{n}_q \lambda_n + M^{-1} H_t(q) \lambda_t$. The generalized friction cone is the cone generated by $\mathbf{n}_q = \frac{1}{m}(0, 1, -\frac{3}{l} \cos(\theta))^T$ and $\pm \mu M^{-1} H_t(q)$, $H_t(q) = M(1, 0, \frac{3}{l} \sin(\theta))^T$, $M = \operatorname{diag}(m, m, I)$, with the edges $e^\pm = \mathbf{n}_q \pm \mu M^{-1} H_t(q)$. It is not symmetric around \mathbf{n}_q , and $\mathbf{n}_q^T M e^+ = \nabla f(q)^T e^+ = B(\theta, \mu)$ in (5.175) so that the generalized cone may dip below the tangent hyperplane $T(q)$, this reflects normal/tangential couplings as in Equation (6.30). This is depicted in Figure 3.

- Page 352, Section 5.6.4, line 18: replace [755, Theorem 1] by [1328, Theorem 1].
- Page 352, Section 5.6.4: the article [11] is worth reading.
- Pages 367 and 430 (Sections 5.7.3.5 and 7.3.2): a (θ, γ) time stepping scheme is used in [12] to calculate periodic solutions of set-valued Lur'e systems (as in Figure 2.2 but with a feedback setvalued nonlinearity of the more general form $(w, \lambda) \in \mathcal{R}$). After discretization a mixed quadratic complementarity problem (MQCP) is constructed. State jumps are incorporated in the problem (remind that LCS may have state discontinuities, see Section 5.4.4.3). The period, the state and the multiplier λ are unknowns of the MQCP. A MQCP is a complementarity problem of the form: Find z, w, v such that

$$\begin{aligned} \varphi(z) + Mz + q &= w - v \\ l \leq z \leq u, (z - l)^T w &= 0, (u - z)^T v = 0 \end{aligned} \quad (1)$$

where $\varphi(\cdot)$ is a vector of quadratic forms in z . The solver PATH is used to solve the discretized MQCP.

- Page 363, Section 5.7.3.2: an interesting application of the NSCD method is in [24] that deals with collapse mechanism of ancient stone arches. Though the NSCD method (the Moreau-Jean algorithm in Section 5.7.3.1) has several shortcomings (like a simplistic impact law as explained in Example 5.6 page 275, see also Section 6.3.3 and the comments page 411), it is interesting for complex systems with many degrees of freedom and unilateral contacts and seems to encapsulate essential modeling features in this case. For a finer analysis of stacked blocks dynamics under base excitation, one should certainly use more sophisticated models like LZB.
- Page 384: it is shown that varying the stiffness ratio γ in the 3-ball system, changes a lot the impact outcome, and this is also true when the mass ratios are varied (the kinetic angle between the two constraints surfaces). This is also true for the 2-ball system hitting a rigid wall (take $m_3 = +\infty$ in Figure 6.5 page 383). The analysis in [27] shows that the mass ratio and the stiffness ratio have a great influence on the kinematic CoR, which varies between 0.2 and 1 (the possibility of several impacts before definitive separation -a kind of micro-collisions effect-between the first ball and the wall is taken into account¹). For the 2-ball system hitting a wall, the kinematic CoR is defined as $-\frac{v(t_f)}{v(t_0)}$ where $v = \frac{m_1 v_1 + m_2 v_2}{m_1 + m_2}$ is the center of mass velocity, t_0 is the time of the first impact, t_f is the time of the last impact before complete separation of the 2-ball system and the wall. Thus depending on these ratios, the system made of the two beads (which we can see as an approximation of the flexibilities in a rigid body like a rod) will rebound with a low or a high velocity. The apparently loss kinetic energy is in fact transformed into potential energy stored in the system's spring under the form of vibrations that persist after the impact is ended. This is therefore also quite related to Sections 4.2.4 and 4.4 material. It is also interesting to compare this result to Theorem 4.1 page 238, which stipulates that an elastic rod that collides a wall with zero external force, has $e_n = 1$. Thus the 2-ball system is not in general a good approximation of the infinite dimensional model. However the results in [27, Figure 2a] show that with equal masses and equal stiffnesses, then $e_n \approx 1$. This is extended to N -ball systems (see also [28, 29]). One assumption that is made in these studies, and might make the analysed chains behaviour different from an elastic rod impacting axially a wall, is that it is assumed that the first (colliding) ball reverses its velocity instantaneously [29].
- Page 394 (*relations between Moreau's impact law in (5.60) (5.61), and the restitution mapping in (6.44) (6.45)*). Here I also refer to the reference [210, Section 3.1.1], with some inaccuracies in Equation (44). Let $\mathcal{I}(q(t))$ be the index set of active constraints at position $q(t)$. Moreau's law states that $\dot{q}(t^+) = \dot{q}(t^-) - (1 + e_n)\text{proj}_{M(q(t))}[N(q(t)); \dot{q}(t^-)]$, see (5.60). Clearly if $\dot{q}(t^-)$ is in the interior of $N(q(t))$ then $\dot{q}(t^+) = -e_n \dot{q}(t^-)$. If this is not the case, one has to project $\dot{q}(t^-)$ onto the normal cone, which is a polyhedral cone generated by the normals $\mathbf{n}_{q,i}$, $i \in \mathcal{I}(q(t))$. In case $N(q(t))$ is a so-called *latticeal* cone, then the material in [210, Section 3.1.1] is correct. We recall that $N(q(t))$ is a latticeal cone if $\dim(q(t)) = \text{card}(\mathcal{I}(q(t)))$, in other words the number of active constraints is equal

¹In [27] this is called multiple impacts, however in our terminology multiple impacts are simultaneous collisions, not a sequence of separated collisions.

to the dimension of $q(t)$ (the configuration space), and the active constraints (hence the vectors $\mathbf{n}_{q,i}$, $i \in \mathcal{I}(q(t))$) are independent (see Németh and Németh, How to project onto an isotone projection cone, Linear Algebra and its Applications, vol.433, 41-51, 2010). In this case the projection of $\dot{q}(t^-)$ onto $N_{\Phi_u^M}^M(q)$ in [210, Section 3.1.1, line 8 after (43)], is correct according to Theorem 2 in Németh and Németh.

One difference between the impact law in (6.44) (6.45), and Moreau's impact rule, is first on the choice of the vectors \dot{q}_{norm} and \dot{q}_{tan} . This explains some discrepancies between both models, as demonstrated for instance on the rocking block problem, see [228, Section 3.4] which shows that with a specific choice of $\dot{q}_{\text{norm},1}$ and $\dot{q}_{\text{norm},2}$, rocking motion is possible only if off-diagonal terms in the restitution matrix in (6.45) are introduced, whatever the kinetic angle value. On the contrary Moreau's law allows for rocking in some situations when the kinetic angle between the two active constraints, is larger than $\pi/2$, see [31].

In practice one uses the equivalent form of Moreau's law in (5.66) and solves a LCP or a mLCP. Using (5.67) and assuming that $D_u(q(t_k)) > 0$, it is easy to construct a LCP with unknown $W(tk) \triangleq U_n(t_k^+) + \mathcal{E}_{\text{nn}}U_n(t_k^-)$:

$$0 \leq W(t_k) \perp D_u(q(t_k))^{-1}W(t_k) - D_u(q(t_k))^{-1}(I_m + \mathcal{E}_{\text{nn}})U_n(t_k^-) \geq 0. \quad (2)$$

This LCP always has a unique solution. If $D_u(q(t_k))^{-1}(I_m + \mathcal{E}_{\text{nn}})U_n(t_k^-) < 0$, then $U_n(t_k^+) + \mathcal{E}_{\text{nn}}U_n(t_k^-) = 0$ which gives Newton's law at each contact with CoR e_n if $\mathcal{E}_{\text{nn}} = \text{diag}(e_n)$ (see Proposition 5.15 for the link between Moreau's impact law and Newton's law at each contact with complementarity, see also the seminal reference [454]). The next step is to write down Moreau's law when $\dot{q}(t^-)$ is not in the interior of $N(q(t))$, but has to be projected on it. When the constraints are not independent, one can still use a numerical solver that computes a solution for LCPs with positive semi-definite matrices (like Lemke's algorithm).

- Page 398, line 2: choosing
- Page 400, line just above Proposition 6.6: replace $\bar{M}(M(q, \mu, v_t))$ by $\bar{M}(q, \mu, v_t)$.
- Page 406, line 7 after (6.68): $\delta_j(p_{f,j}) \leq 0$ (here we assume that compression occurs with positive indentation velocity $\delta_j > 0$ and expansion occurs with negative indentation velocity $\delta_j < 0$), in agreement with Figure 6.6. Thus indentation increases during compression and decreases during expansion (or restitution).
- Page 407: Notice that Equations (6.71) (6.72) can be rewritten in a differential form $\frac{dE_j}{dp_j}(p_j) = \delta_j(p_j)dp_j$ and similarly for (6.72), so that the whole LZB dynamics is a first-order dynamics with augmented state variable (the potential energy becomes a state variable). Thus the calculation of the positions (assumed to be constant in the LZB approach) is not at all needed to integrate the system (see reference 929 Equations (4.42) and (4.43) where a midpoint rule is used to approximate the potential energies). Notice further that (6.72) indeed stipulates that according to the energetic constraint $W_{e,j} = -e_{*,j}^2 W_{c,j}$ (using (4.159)), then at the end of the impact $E_j(p_{f,j}) = 0$.
- Page 407 Section 6.3.2: another interesting application of the LZB model is in [26].
- Page 415, line 8: drop the "be".
- Page 429, Equation (7.18): replace e in σ_1 and σ_2 by e_n .
- Page 452, Equation (7.51): $0 \leq f(q^*) \perp \lambda_{n,u}^* \geq 0$.
- Page 456, Equation (7.62), last two lines: $\sum_{k \in [k_0, k_1]}$ instead of $\sum_{k \in [k_0, k_1]}$ which might let one think that only the two values k_0 and k_1 are taken into account.

- Pages 457-458: The stability (finite-time convergence to a fixed point, plus Lyapunov stability) of simple systems with set-valued terms encompassing Coulomb's friction with constant normal force, is analysed in [22]. The discretisation of the same dynamics is studied in [23], where it is shown that the sequence of discrete solutions converges in a finite number of steps to its limit. This is quite similar to the results mentioned in Section 5.7.3.7 about implicit discrete-time sliding mode control (though control has its own peculiarities like the fact that one wants to study robustness with respect to parameter uncertainties, unmatched disturbances, more complex attractive surfaces, *etc*). It may also be seen as a generalization of the case treated in Remark 5.33 pages 362-363.
- Pages 457-458: it is clear that the fixed points of a system with unilateral contact and Coulomb friction are also solutions of a generalized equation, extending (7.51). As said page 458, in general uniqueness of the equilibrium is lost. Consider for instance (5.162) page 336. For this system the equilibria $(q, \dot{q}) = (q^*, 0)$ satisfy the generalized equation:

$$\begin{cases} \begin{pmatrix} 0 \\ 0 \end{pmatrix} = \begin{pmatrix} \sin(\alpha) \\ \cos(\alpha) \end{pmatrix} \lambda_n^* + \begin{pmatrix} -\cos(\alpha) \\ \sin(\alpha) \end{pmatrix} \lambda_t^* + \begin{pmatrix} F_x \\ 0 \end{pmatrix} \\ 0 \leq f(q^*) \perp \lambda_n^* \geq 0 \\ \lambda_t^* \in -\mu \lambda_n^* \text{sgn}(0) \end{cases} \quad (3)$$

with $\text{sgn}(0) = [-1, 1]$. It is noteworthy that usually the generalized equation for equilibria and the generalized equation for sticking contacts, are not the same (in this example they are the same because sticking contact implies that the system does not move, and conversely). Also this is different from the generalized equation in (5.165) which is obtained from the acceleration Coulomb's friction model.

- Page 462: Chapter 7 could be nicely completed with the study in [32] which analyzes the contact stability of a simple system, with a force feedback controller, and subject to delay in the force feedback. These theoretical results were experimentally validated by Tornambé in [33].
- Page 531, Section 8.5.2: controllability of juggling systems (with the important assumption that the robot dynamics in (8.74) has much bigger mass than the object, so that \dot{q}_2 is continuous at impacts) as well as their stabilization, is studied in [30].
- Page 551, Lemma B.1: it is more appropriate to write $f : \text{dom}(f) \subseteq \mathbb{R}^n \rightarrow \mathbb{R} \cup \{+\infty\}$ (though one might understand that \mathbb{R} contains the infinity).
- Page 552, figure B.2: in the first figure on the left, replace $f_\lambda(x)$ by $-f_\lambda(x)$. The Moreau-Yosida approximation is a convex function. It becomes obvious also from this figure, that the function $-f_\lambda(\cdot)$ represents the potential energy function of a unilateral spring, and has to be compared with the indicator function which represents the potential energy associated with complementarity conditions (which are a particular contact model).
- Page 553: For better clarity replace the set Φ in the paragraph after (B.12), by \mathcal{C} .
- Page 560, Section B.2.2: line 3: replace (5.35) by (5.35), line 6: replace Definition 5.34 by (5.34).
- Pages 561-562, about prox-regular sets. Characterizations of finitely represented sets which are prox-regular are given in [18, Theorems 3.1, 4.1], in addition to Theorem B.5. An interesting result about the preservation of prox-regularity under an inverse linear transformation $S' = H^{-1}(S) = \{z | Hz \in S\}$, is in [19, Lemma 2.7] (reference 1181 in the book's bibliography). If $S \subset \mathbb{R}^l$ is r -prox-regular, and if S is in the range space of $H : \mathbb{R}^n \rightarrow \mathbb{R}^l$,

then S' is r' -prox-regular with $r' = \frac{r\sigma_H^+}{\|H\|^2}$, where σ_H^+ is the least positive singular value of H and $\|H\|$ is an induced matrix norm. An extension is in [18, Corollary 6.5].

- Page 622, index for G , add for Gauss's principle: systems with friction, 332.

References

1. A. Curnier, Unilateral Contact: Mechanical Modelling. In: New Developments in Contact Problems, P. Wriggers and P.D. Panagiotopoulos (Eds.), CISM Courses and Lectures no 384, Springer Wien New York, pp.1-54, 1999
2. P. Moylan, Dissipative Systems and Stability, Newcastle, NSW, Australia, <http://www.pmoylan.org>
3. Li, C., Xu, W., Feng, J., Wang, L.: Response probability density functions of Duffing-Van der Pol vibro-impact system under correlated Gaussian white noise excitation. *Physica A* **392**, 1269–1279 (2013)
4. Rong, H., Wang, X., Xu, W., Fang, T.: Subharmonic response of a single-degree-of-freedom nonlinear vibroimpact system to a randomly disordered periodic excitation. *Journal of Sound and Vibration* **327**, 173–182 (2009)
5. Feng, J., Xu, W., Rong, H., Wang, R.: Stochastic responses of Duffing-Van der Pol vibro-impact system under additive and multiplicative random excitations. *Int. J. of Non-Linear Mechanics* **44**, 51–57 (2009)
6. Feng, J., Xu, W., Wang, R.: Stochastic responses of vibro-impact Duffing oscillator excited by additive Gaussian noise. *Journal of Sound and Vibration* **309**, 730–738 (2009)
7. G. Hu, Z. Hu, B. Jian, L. Liu, H. Wan, On the determination of the damping coefficient of nonlinear spring-dashpot system to model Hertz contact for simulation by discrete element method, Information Engineering (ICIE), 2010 WASE International Conference on, vol.3, pp.295-298, 14, 15 August 2010
8. Kacianauskas, R., Kruggel-Emden, H., Zdancevicius, E., Markauskas, D.: Comparative evaluation of normal viscoelastic contact force models in low velocity impact situations. *Advanced Powder Technology* (2016). doi:[10.1016/j.apt.2016.04.031](https://doi.org/10.1016/j.apt.2016.04.031)
9. Nguyen, N.S., Brogliato, B.: Shock dynamics in granular chains: numerical simulations and comparisons with experimental tests. *Granular Matter* **14**(3), 341–362 (2012)
10. N.S. Nguyen, B. Brogliato, *Multiple Impacts in Dissipative Granular Chains*, Springer Verlag, Lecture Notes in Applied and Computational Mechanics vol.72, 2014
11. Champneys, A., Varkonyi, P.: The Painlevé paradox in contact mechanics. *IMA Journal of Applied Mathematics* **81**, 538–588 (2016)
12. V. Sessa, L. Iannelli, F. Vasca, V. Acary, A complementarity approach for the computation of periodic oscillations in piecewise linear systems, *Nonlinear Dynamics*, DOI: [10.1007/s11071-016-2758-5](https://doi.org/10.1007/s11071-016-2758-5)
13. Fetecau, R.C., Mardsen, J.E., Ortiz, M., West, M.: Nonsmooth Lagrangian mechanics and variational collision integrators. *SIAM J. Applied Dynamical Systems* **2**(3), 381–416 (2003)
14. Kojima, M., Saigal, R.: On the number of solutions to a class of linear complementarity problems. *Mathematical Programming* **17**, 136–139 (1979)
15. Paoli, L.: Vibro-impact problems with dry friction-Part I: Existence result. *SIAM J. Math. Anal.* **47**(5), 3285–3313 (2015)
16. Paoli, L.: Vibro-impact problems with dry friction-Part II: Tangential contacts and frictional catastrophes. *SIAM J. Math. Anal.* **48**(2), 1272–1296 (2016)
17. F. Génot, B. Brogliato, New results on Painlevé paradoxes, INRIA Research Report 3366, February 1998, <https://hal.inria.fr/inria-00073323>
18. Adly, S., Nacry, F., Thibault, L.: Preservation of prox-regularity of sets with applications to constrained optimization. *SIAM J. Optim.* **26**(1), 448–473 (2016)

19. Tanwani, A., Brogliato, B., Prieur, C.: Stability and observer design for Lur'e systems with multivalued, non-monotone, time-varying nonlinearities and state jumps. *SIAM J. Control and Optimization* **56**(2), 3639–3672 (2014)
20. Adly, S., Goeleven, D., Le, B.K.: Stability analysis and attractivity results of a DC-DC Buck converter. *Set-Valued Var. Anal.* **20**, 331–353 (2012)
21. Adly, S., Cibulka, R., Massias, H.: Variational analysis and generalized equations in electronics. *Set-Valued Var. Anal.* **21**, 333–358 (2013)
22. S. Adly, H. Attouch, A. Cabot, Finite time stabilisation of nonlinear oscillators subject to dry friction, in *Nonsmooth Mechanics and Analysis*, P. Alart, O. Maiconneuve, R.T. Rockafellar (Eds.), Springer, Chapter 24, pp.289-304, 2006
23. Baji, B., Cabot, A.: An inertial proximal algorithm with dry friction: finite convergence results. *Set-Valued Analysis* **9**, 1–23 (2006)
24. Lancioni, G., Gentilucci, D., Quagliarini, E., Lenci, S.: Seismic vulnerability of ancient stone arches by using a numerical model based on the Non-Smooth Contact Dynamics method. *Engineering Structures* **119**, 110–121 (2016)
25. Xiao, H., Shao, Y., Brennan, M.J.: On the contact stiffness and nonlinear vibration of an elastic body with a rough surface in contact with a rigid flat surface. *European Journal of Mechanics A/Solids* **49**, 321–328 (2015)
26. Z. Zhao, C. Liu, T. Chen, Docking dynamics between two spacecrafts with APDSes, *Multibody System Dynamics*, 2016
27. Ruan, H.H., Yu, T.X.: The unexpectedly small coefficient of restitution of a two-degree-of-freedom mass-spring system and its implications. *International Journal of Impact Engineering* **88**, 1–11 (2016)
28. Basile, A.G., Dumont, R.S.: Coefficient of restitution for one-dimensional harmonic solids. *Phys. Rev. E* **61**(2), 2015–2023 (2000)
29. Nagahiro, S.I., Hayakawa, Y.: Collision of one-dimensional nonlinear chains. *Physical Review A* **67**, 036609 (2003)
30. Lynch, K.M., Black, C.K.: Recurrence, controllability, and stabilization of juggling. *IEEE Transactions on Robotics and Automation* **17**(2), 113–124 (2001)
31. A.I. Giouvanidis, E.G. Dimitrakopoulos, Modelling contact in rocking structures with a non-smooth dynamics approach, *ECCOMAS Congress 2016, VVII European Congress on Computational Methods in Applied Sciences and Engineering*, M. Papadrakakis, V. Papadopoulos, G. Stefanou, V. Plevris (eds.), Crete Island, Greece, 5-10 June 2016
32. Niculescu, S.I., Brogliato, B.: Force measurement time-delays and contact instability phenomenon. *European Journal of Control* **5**, 279–289 (1999)
33. Tornambé, A.: Discussion on “Force measurement time-delays and contact instability phenomenon”. *European Journal of Control* **5**, 290–292 (1999)